Investigation and identification of let-7a related functional proteins in gastric carcinoma by proteomics

Yimin Zhu[a], Xingyuan Xiao[b], Lairong Dong[a] and Zhiming Liu[c, *]

[a]*Department of Oncology, The Second Hospital of Jiaxing, Jiaxing, China*
[b]*Department of General Surgery, The First People's Hospital of Kunshan, Kunshan, China*
[c]*Gastrointestine and Gland Surgery Division, The First Affiliated Hospital of Guangxi Medical University, Nanning, China*

Abstract. MicroRNAs are small noncoding RNA molecules that control expression of target genes. Our previous studies show that let-7a decreased in gastric carcinoma and that up-regulation of let-7a by gene augmentation inhibited gastric carcinoma cell growth both *in vitro* and *in vivo*, whereas it remains largely unclear as to how let-7a affects tumor growth. In this study, proteins associated with the function of let-7a were detected by high throughout screening. The cell line of SGC-7901 stably overexpressing let-7a was successfully established by gene cloning. Two-dimensional gel electrophoresis (2-DEy was used to separate the total proteins of SGC-7901/let-7a, SGC-7901/EV and SGC-7901, and PDQuest software was applied to analyze 2-DE images. Ten different protein spots were identified by MALDI-TOF-MS, and they may be the proteins associated with let-7a function. The overexpressed proteins included Antioxidant protein 2, Insulin–like growth factor binding protein 2, Protein disulfide isomerase A2, C-1-tetrahydrofolate synthase, Cyclin-dependent kinase inhibitor1 (CDKN1) and Rho–GTPase activating protein 4. The underexpressed proteins consisted of S-phase kinase-associated protein 2 (Spk2), Platelet membrane glycoprotein, Fibronectin and Cks1 protein. Furthermore, the different expression levels of the partial proteins (CDKN1, Spk2 and Fibronectin) were confirmed by western blot analysis. The data suggest that these differential proteins are involved in a novel let-7a signal pathway and these findings provide the basis to investigate the functional mechanisms of let-7a in gastric carcinoma.

Keywords: Proteomics, miRNA, gastric carcinoma

1. Introduction

MicroRNAs (miRNAs) are a class of naturally occurring small noncoding RNAs that regulate gene expression by targeting mRNAs for translational repression or cleavage [1, 2]. They bind through par-

tial sequence homology to the $3'$-untranslated region ($3'$-UTR) of target genes. Because of this unique feature, a single miRNA has multiple targets. Thus, miRNAs could regulate a large fraction of protein-coding genes, and as high as 30% of all genes could be miRNA targets [3]. As a new layer of gene regulation mechanism, miRNAs have diverse functions, including the regulation of cellular differentiation, proliferation, and apoptosis [4, 5]. However, although miRNAs have been the subject of extensive research in recent years, the molecular basis of miRNA-mediated

*Corresponding author: Zhiming Liu, Gastrointestine and Gland Surgery Division, The First Affiliated Hospital of Guangxi Medical University, 6th Shuangyong Road, Nanning 530021, P.R. China. Tel.: +86 771 5356738; Fax: +86 771 5356738; E-mail: zym330422@163.com.

gene regulation and the effect of these genes on tumor growth remain largely unknown because of our limited understanding of miRNA-target genes. Evidence suggests that perfect seed pairing may not necessarily be a reliable predictor for miRNA-target interactions [6], which may explain why many predicted target sites are nonfunctional. A recent study also suggests that there may be at least three types of miRNA-mRNA interactions in mammals [7]. Hence, with few exceptions, a large portion of the physiologic targets for miRNAs remain to be identified or verified experimentally.

Gastric carcinoma is the second most prevalent cancer and there are still 0.3 million deaths from gastric carcinoma annually in China. One particular microRNA, let-7, has been reported as a novel candidate of tumor suppressor genes involved several cancers. In our previous study, it was found that reduced let-7a was one of the earliest biochemical events associated with the progression of gastric mucosa cancerization [8]. Therefore, we then conducted a study to determine the influence of let-7a overexpression on cell proliferation or the cell cycle in an *in vitro* and *in vivo* cell model for gastric carcinoma. The results demonstrated that a lentiviral vector was capable of upregulating let-7a, resulting in impressive anticancer effects [9, 10]. Based on our results, overexpression of the let-7a gene provides a potential therapeutic approach for the management of gastric carcinoma. Our studies strongly support the notion that let-7 functions as a tumor suppressor miRNA in gastric carcinoma while the molecular mechanism used by let-7 to repress tumor formation is largely unknown.

Proteomics is an effective platform to globally detect and characterize proteins. Comparative proteomic approach is the main strategy of proteomics to analyze and compare the differentially expressed proteins [11, 12]. On the other hand, gene augmentation is an important method in treating cancers. Thus, we used gene cloning to overexpress let-7a in the human gastric carcinoma cell line SGC-7901 which was named SGC-7901/let-7a. SGC-7901 cells transduced with empty lentiviral vectors were used as the negative control group, which was named SGC-7901/EV. The parental SGC-7901 cells were used as a blank control group. A comparative proteomic approach was performed to identify the differential proteins among SGC-7901/let-7a and control cells. In our study, we used two-dimensional gel electrophoresis (2-DE) to detect the differentially expressed proteins in SGC-7901/let-7a and control cell

lines. The differentially expressed proteins among the three cell lines were identified by matrix-assisted laser desorption/ionization time-of-flight mass spectrometry (MALDI-TOF-MS). Furthermore, the relationships of partial identified differential proteins with let-7a in SGC-7901 were studied by Western blot analysis. The results presented here will provide clues for further study of functional mechanism of let-7a in treating human gastric carcinomas.

2. Materials and methods

2.1. Cell culture

Human gastric carcinoma cells SGC-7901, and human embryonic kidney (HEK) 293T cells were cultured in Dulbecco's modified Eagle's medium (DMEM, Gibco) with 10% heat-inactivated FBS, 2 mM L-glutamine, 100 U/ml penicillin and 100 μg/ml streptomycin at 37°C in a humidified atmosphere of 5% CO_2.

2.2. Plasmid construction

The DNA sequence of let-7a was obtained from Gene Bank (ID No. NM_0062). The primers (forward primer, 5′-AGGATCC AAAGGTGGTGGTAAGA GGGTGAT3′; reverse primer, 5′-AGTCGAC ATA AGACAAGAAGCAAAAGGTTT-3′) were designed to amplify the entire coding sequence of let-7a and produced an amplified product of 600 bp. The rounds of PCR were performed according to the TaKaRa LA Taq data sheet. After PCR, 2 μl of the amplified product was electrophoresed in 1% agarose gelatin gels buffered with 1× TBE. The plasmid of Pwpxl-MOD2, a gift of Dr. Liu (Shanghai Jiaotong University), was used to construct the let-7a expression vector. The PCR product and Pwpxl-MOD2 were digested with BamHI and SalI. The fragment was isolated from agarose gel and ligated into the cut vector to form Pwpxl-MOD2-let-7a, which was then transfected into 293T cells. While the negative control plasmid Pwpxl-MOD2 just was not digested and ligated any oligonucleotide. The transfer plasmid Pwpxl-MOD2-let-7a expressing let-7a shRNA and the control negative plasmid Pwpxl-MOD2 were constructed for packaging lentiviral vectors. Both of them can express enhanced green fluorescent protein (EGFP).

2.3. Generation and titer of lentivirus

Lentiviral vector supernatant was produced by four-plasmid cotransfection in the HEK 293T transient system. Briefly, 20 μg Pwpxl-MOD2-let-7a (transfer plasmid) and 15 μg pMDlg-Prre, 10 μg pRsv-REV, pMD2 G 7.5 μg (packaging plasmids)were used to cotransfect HEK 293T cells using calcium phosphate co-precipitation. 3.0×10^6 293T cells were seeded in 10-cm cell culture dishes, and allowed to reach a con-fluence of 70–80% for transfection. Culture medium was replaced 16–18 h after transfection with 15 ml of 10% FCS DMEM per dish. Viral supernatant was har-vested 72 h after transfection and filtered through a 0.45-μm cellulose acetate filter, then ultracentrifuged at 50,000 g at 4°C for 2 h. The viral pellet was resus-pended in serum-free DMEM, divided into aliquots and frozen at –70°C. The control lentiviral vector super-natant was made similarly. The functional titer of virus in SGC-7901 cells was determined by *in vitro* transduc-tion and flow cytometry(FCM) analysis [13].

2.4. Establishment of stable overexpression lines

SGC-7901 cells were transduced with specific or empty lentiviral vectors using a multiplicity of infec-tion of 5 and selected for stable integrants using EGFP reporter gene. Briefly, the transduced SGC-7901 cells were maintained in culture medium for four to five passages until EGFP expression was stable; the trans-duced cells were trypsinized, diluted to 10 cells/ml, and 100 μl of cells were seeded in each well of a 96-well plate. After 10 days of incubation, the single colony strongly expressing EGFP was selected under a flu-orescent microscopy. The EGFP-positive cells were named SGC-7901/*let-7a*, SGC-7901/EV, respectively. Passages 10–20 were used in the experiments. There was no significant change in morphological characteri-zation from passage 10 to 20. Subsequently, more than 98% transduced cells were found to strongly express EGFP using fluorescent microscopy (Fig. 1). Those cells expressing EGFP were selected through FCM as stable overexpression lines.

2.5. Real-time RT-PCR analysis of let-7a

Total RNA was isolated from cultured cells using Trizol reagent (Invitrogen). Let-7a was quantified with real-time RT-PCR. Primer sequences were designed using the Primer Express software pro-gram (PE Applied Biosystems): forward primer: GCCGCTGAGGTAGTAGGTTGTA; reverse primer: GTGCAGGGTCCGAGGT. 18sRNA was used as an endogenous control. The reaction was performed in a volume of 25 μl containing oligonucleotide primers (2 μl each), cDNA template (0.5 μl) and SYBR Green mix (25 μl) in duplicate. The amplifications were per-formed in the ABI Prism 7000 Sequence Analyzer using the following cycle program: 95°C for 5 min, 95°C for 20 s, 50°C for 15 s, 68°C for 20 s followed by 40 cycles and then 68°C for 10 min. The relative expression level of the let-7a gene was calculated by comparing the threshold cycle (Ct) values of samples to that of the reference (SGC-7901). The Ct values for each reaction were determined using Taq-Man SDS analysis software. For each sample tested, the duplicate Ct values were averaged, Accordingly, $^{\Delta}Ct$ = (mean of SGC-7901/*let-7a* Ct) – (the mean of 18sRNA Ct), and $^{\Delta\Delta}Ct = {}^{\Delta}Ct$ (SGC-7901/*let-7a*) – $^{\Delta}Ct$ (SGC-7901). The relative gene expression in a particular sample was then given by the relative amount of the target: $2^{-\Delta\Delta Ct}$ value [14] (Fig. 2).

2.6. 2-DE

Monolayer cultures of three cell lines SGC-7901/let-7a, SGC-7901/EV, and SGC-7901 were harvested, and lysed in lysis buffer (7 M urea, 2 M thiourea, 100 mM DTT, 4% Chaps, 40 mM Tris, 2% Pharmalyte, 1 mg/ml DNase I). After being incubated at 37°C for 1 h, the lysates were centrifuged at 15000 rpm for 30 min at 4°C. The supernatant was transferred and the concen-tration of the total proteins was determined using 2D Quantification kit (Amersham Biosciences). Triplicate gels were made for each cell line and a total amount of 1.0 mg of protein per gel was analyzed. Protein sam-ples were diluted to 450 μl with rehydration solution [7 M urea, 2 M thiourea, 0.2% DTT, 0.5% (v/v) Ph 4–7 IPG buffer (Amersham Biosciences), and trace bro-mophenol blue] and applied to IPG strips (pH 4–7 L, 240 mm × 3 mm × 0.5 mm, Amersham Biosci-ences) by 24 h rehydration at 30 V. Then proteins were focused successively for 1 h at 500 V, 1 h at 1000 V and 8.5 h at 8000 V to give a total of 68 kVh on an IPGphor (Amersham Biosciences). Focused IPG strips were equilibrated for 15 min in a solution (6 M urea, 2% SDS, 30% glycerol, 50 mM Tris–HCl, pH 8.8 and 1% DTT), and then for an additional 15 min in the same
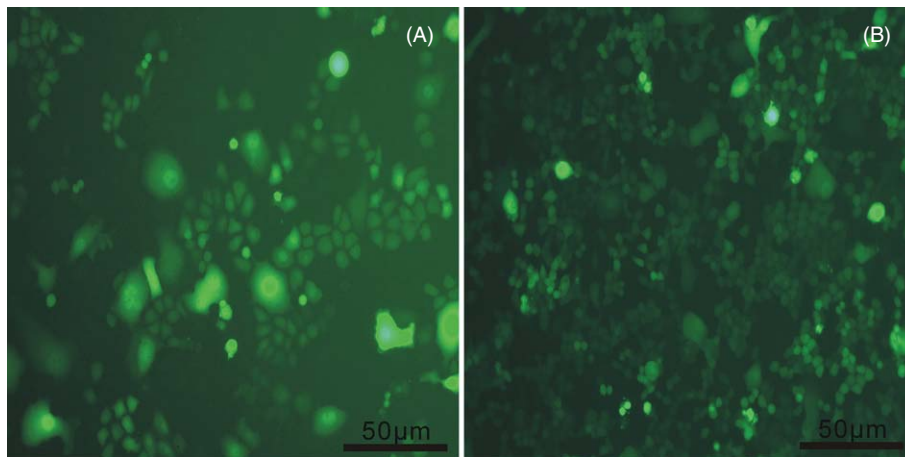
Fig. 1. SGC-7901 transduced with lentiviral vectors. (A) Selected cells (parental SGC-7901) were transduced with let-7a lentiviral vectors at a multiplicity of infection of 5 and selected for stable integrants using EGFP reporter gene. Original magnification: ×200. (B) Selected cells (parental SGC-7901) were transduced with empty lentiviral vectors at a multiplicity of infection of 5 and selected for stable integrants using EGFP reporter gene. Calibration bar is 50 μm for both panels.
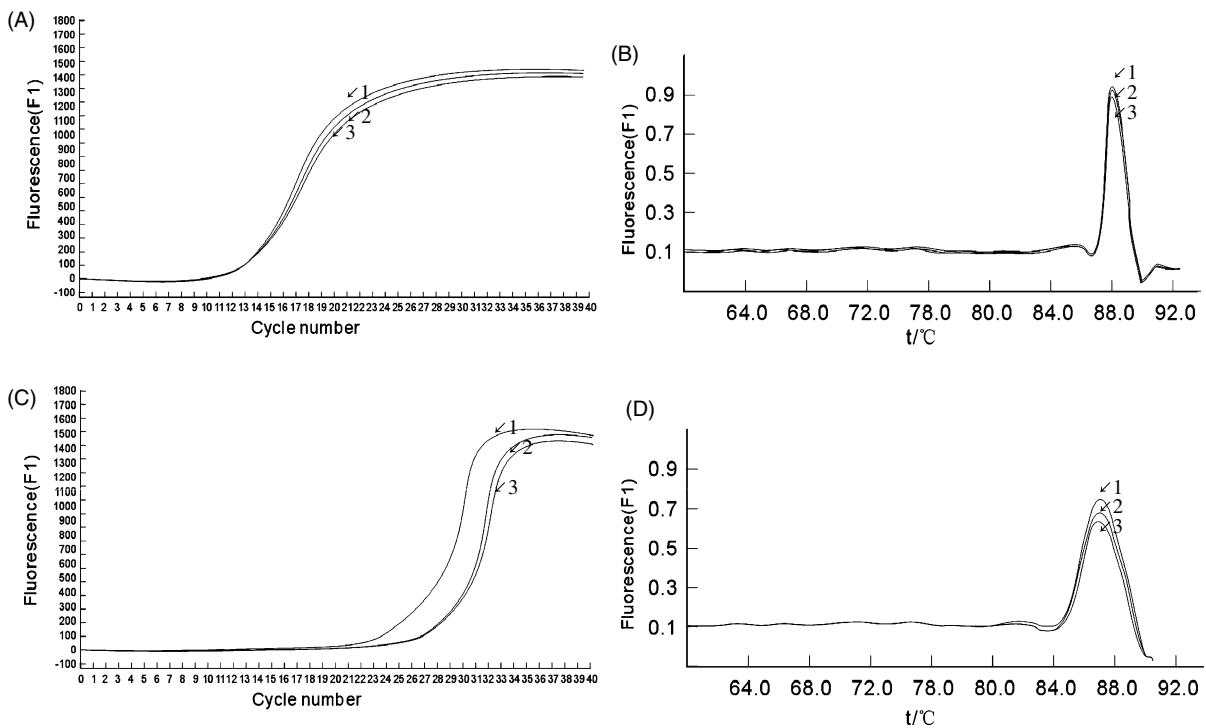

Fig. 2. Representative real-time quantitative RT-PCR analysis for of let-7a level. The expression level of let-7a was examined and was normalized to that of 18 S RNA. (A) Graph shows that 18 S RNA among SGC-7901/let-7a, SGC-7901/EV and SGC-7901 cell lines has very little difference. (C) Graph showed that let-7a significantly increased in the SGC-7901/let-7acell line. (B) and (D) Graph showed the melt curve of representative PCR products of 18 S RNA and let-7a respectively. 1: SGC-7901/let-7a; 2:SGC-7901/EV; 3: SGC-7901.

solution except that DTT was replaced by 2.5% iodoac-etamide (Sigma–Aldrich). After equilibration, second-dimension sodium dodecyl sulfate–polyacrylamide gel electrophoresis (SDS–PAGE) was performed on the Ettan DALT II system (Amersham Biosciences). After SDS–PAGE, the Blue Silver staining method, a modified Neuhoff's colloidal coomassie blue G-250 stain (Amersham Biosciences), was used to visualize the protein spots in the 2-DE gels [15].

2.7. Gel scanning and image analysis

The stained 2-DE gels were scanned with Magic-Scan software on Imagescanner (maximum resolution 9600×9600 dpi) (Amersham Biosciences), and analyzed using PDQuest system (Bio-Rad Laboratories, Hercules, CA, USA) according to the protocols provided by the manufacturer. To minimize the contribution of experimental variations, three separate gels were prepared for each cell line. The gel spot pattern of each gel was summarized in a standard after spot matching. Thus, we obtained one standard gel for each cell line. Spot intensities were quantified by calculation of spot volume after normalization of the image using the total spot volume normalization method multiplied by the total area of all the spots. The change index was defined as the ratio between the spot percentage relative volumes in SGC-7901/let-7a, SGC-7901/EV, and SGC-7901 cell lines. All indexes were calculated based on the mean of the spot intensities of all nine gels, with standard deviations. Proteins were classified as being differentially expressed between the two cell lines when spot intensity showed a difference $\geq$5-fold variation in SGC-7901/let-7a, SGC-7901/EV in comparison to SGC-7901. Significant differences in protein expression levels were determined by Student's *t*-test with a set value of $P < 0.05$.

2.8. Protein identification by MALDI-TOF-MS

Selected differential protein spots were excised from preparative gels using punch and in-gel digestion was performed. The gel-spots were washed three times with two-distillation water and destained with fresh solution containing 100 mM NH_4HCO_3 in 50% acetonitrile at 37°C. After drying in a vacuum centrifuge, the gel-pieces were incubated in 10 μl digestion solution consisted of 40 mM NH_4HCO_3 in 9% acetonitrile solution, and 20 μg/ml proteomics grade trypsin (Promega,

USA) for 10–12 h at 37°C. The tryptic peptide mixture was extracted and purified with a Millipore ZipTip C18 column (Millipor, Bedford, MA, USA). The purified tryptic peptide mixture was mixed with containing α-cyano-4-hydroxycinnamic (CCA) (Sigma–Aldrich Co.) matrix solution and vortexed gently. A volume (1 μl) of the mixture CCA matrix was loaded on a stainless steel plate and air-dried, and then was analyzed with Voyager System DE-STR 4307 MALDI-TOF Mass Spectrometer (AppliedBiosystems, Foster City, CA, USA). The standard peptide mixture was spotted at the same time to correct the machine. In peptide mass fingerprint (PMF) map database searching, Mascot Distiller was used to get the monoisotopic peak list from the raw mass spectrometry files. Peptide matching and protein searches against the Swiss-Prot databases were performed using the Mascot search engine (http://www.matrixscience.com/) with a mass tolerance of ±50 ppm.

2.9. Western blot analysis of let-7a related proteins

The cells were harvested from flasks, and lysed in a lysis buffer (50 mM Tris, pH 7.4, 100 mM NaCl, 1 mM $MgCl_2$, 2.5 mM Na_3VO_4, 1 mM PMSF, 2.5 mM EDTA, 0.5% Triton X-100, 0.5% NP-40, 51 g/mL of aprotinin, pepstatin A, and leupeptin) for 60 min on ice, followed by centrifuging at $11000 \times g$ for 15 min at 4°C to remove cell debris. The concentration of proteins was determined using Bradford reagent (Bio-Rad Laboratories). Protein samples (500 μg) were separated on 12.5% SDS–PAGE gels, and transferred to Hybond-P PVDF membranes (Amersham Biosciences, Stockholm, Sweden). After blocking with 5% non-fat dry milk in TBS-T buffer (20 mM Tris, pH 7.6, 100 mM NaCl, 0.1% Tween-20) for 2 h at room temperature, the membranes were respectively probed with 1 : 1000 dilution of anti-CDKN1, anti-Skp2 and anti-Fibronectin (Santa Cruz Biotechnology, CA, USA) overnight at 4°C, and probed with 1 : 1000 dilution of anti-GAPDH (Sigma–Aldrich) to correct for differences in protein loading, followed by incubation in a 1 : 2000 dilution of secondary antibodies conjugated to horseradish peroxidase (Amersham Biosciences) for 1 h at room temperature. Protein bands were detected using ECL detection system (Amersham Biosciences). All of the western immunoblots were performed at least three times.

3. Results

3.1. Overexpression of let-7a in gastric carcinoma cells transduced with let-7a lentiviral vector

The lentiviral-vector-overexpression let-7a gene and control empty vectors were constructed and used to transduce the gastric carcinoma cell line (SGC-7901). Colonies with strong EGFP expression were selected to construct let-7a stable overexpressing cells (Fig. 1). By *in vitro* transduction and flow cytometry (FCM) analysis, results showed that the functional titer of virus was 5.0×10^8 TU/ml. In order to verify the let-7a overexpressing effects, total RNAs were isolated from SGC-7901, SGC-7901/EV and SGC-7901/let-7a cells. We characterized let-7a at the RNA levels by real-time RT-PCR (Fig. 2). The copies of let-7a in SGC-7901/let-7a cells were 9-fold higher than in SGC-7901cells, SGC-7901/EV cells, respectively ($P < 0.001$). There was no significant increase in empty vector-transduced cells, compared to the parental cells (Fig. 3). The overexpression of let-7a with lentiviral vectors was significant and specific. Lentiviral constructs can increase the expression of let-7a gene efficiently.

3.2. 2-D gel analysis of differentially expressed proteins

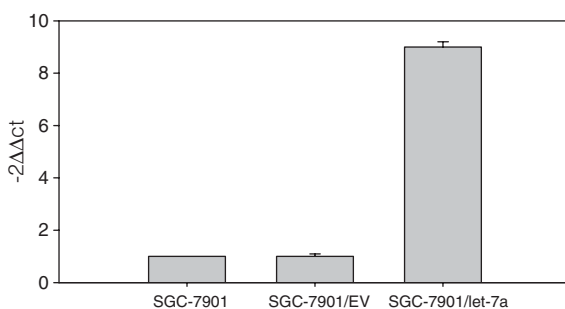To identify the proteins associated with the function of let-7a in SGC-7901, we initiated a comparative

Fig. 3. Real-Time RT-PCR analysis of let-7a in SGC-7901, SGC-7901/EV and SGC-7901/let-7a cells. The relative expression level of the let-7a was calculated by comparing the threshold cycle (Ct) values of samples to that of the reference (SGC-7901). For each sample tested, the three times of duplicate Ct values were averaged, The copies of let-7a in SGC-7901/let-7a cells were 9-fold higher than in SGC-7901cells and SGC-7901/EV cells, respectively ($P = 0.00$). There was no significant increase in SGC-7901/EV cells, comparing to SGC-7901 cells.

proteomic study of SGC-7901/let-7a, SGC-7901/EV, and SGC-7901 cell lines. In the preliminary experiment, 2-DE maps of SGC-7901/let-7a, SGC-7901/EV, and SGC-7901 were performed for several repeated runs. We found that most of the differentially expressed proteins were included in the pH range from 3 to10. To isolate these proteins more efficiently, the narrow pH 3–10 IPG strips for the first dimension were used to better separate the total proteins. In the pH range 3–10, three representative 2-DE maps from SGC-7901/let-7a, SGC-7901/EV, and SGC-7901 are shown in Fig. 4A. For a reliable analysis of protein expression, 2-DE of each cell line was performed in triplicate. The 2-DE patterns of each cell line were highly reproducible and well-resolved. The 2-DE maps of SGC-7901/let-7a, SGC-7901/EV, and SGC-7901 displayed about 1026, 1046 and 1043 protein spots respectively. Maps of SGC-7901/EV and SGC-7901 were similar to each other, while the map of SGC-7901/let-7a was distinguishable from SGC-7901/EV and SGC-7901. Close-ups of the region of the gels showing differential expression proteins between SGC-7901/let-7a, SGC-7901/EV, and SGC-7901 are shown in Fig. 4B. Image analysis revealed that 6 spots (1–6) were specifically upregulated ($\geq$5-fold upregulated; $P < 0.05$) in the SGC-7901/let-7a while 4 spots (7–10) were decreased ($\geq$5-fold downregulated; $P < 0:05$) in comparison with the expression in SGC-7901/EV and SGC-7901.

3.3. Identification of differential expression proteins by MALDI-TOF-MS

The 10 differentially expressed protein spots, marked with the numbers and arrows in Fig. 4A, were excised from coomassie brilliant blue-stained gels, in situ digested with trypsin and analyzed by MALDI-TOF-MS. High-quality PMFs were obtained, and all the 10 differentially expressed protein were identified. The MALDI-TOF mass spectrometry maps of spots 5, 7, 9 are shown in Fig. 5A, B and C, respectively. Their monoisotopic peaks were input into the Mascot search engine to search the Swiss-Prot database and the query results showed that protein spots were Antioxidant protein 2, Insulin–like growth factor binding protein 2, Protein disulfide isomerase A2, C-1-tetrahydrofolate synthase, Cyclin-dependent kinase inhibitor1, Rho-GTPase activating protein 4, S-phase kinase-associated protein 2, Platelet membrane glycoprotein, Fibronectin and Cks1 protein. The
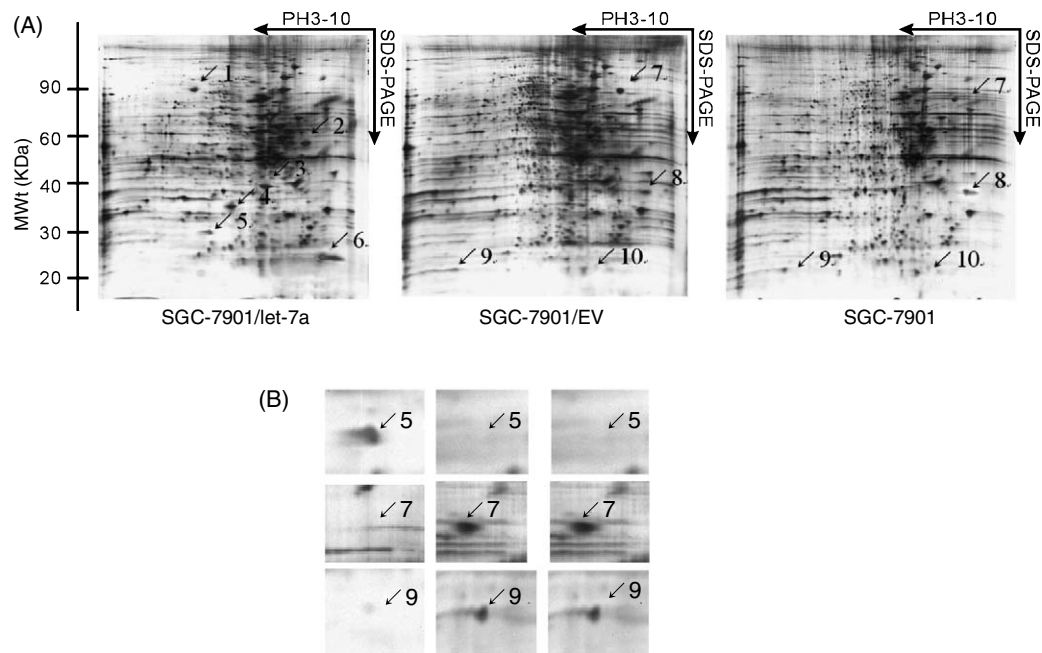
Fig. 4. Representative 2-DE maps of SGC-7901, SGC-7901/EV and SGC-7901/let-7a cell lines. (A) 10 differential expression proteins spots-marked with arrows were identified using 2-DE. (B) Close-up image of partial differential expression protein spots among SGC-7901/let-7a, SGC-7901/EV and SGC-7901 cells.

Table 1

MALDI-TOF-MS identified proteins in SGC-7901/let-7a vs. SGC-7901 and SGC-7901/EV

Spot no.	Protein name	Accession number	Matching	pI	Molecular weight	% Coverage	Classification
1	Antioxidant protein 2	P30041	7/19	8.28	82904	40.9	Metabolism
2	Insulin-like growth factor binding protein 2	P18065	7/13	4.31	50137	42.1	Signal transduction
3	Protein disulfide isomerase A2	Q13087	6/18	6.04	39206	51.5	Metabolism
4	C-1-tetrahydrofolate synthase	P11586	7/23	6.79	34428	65.6	Metabolism
5	Cyclin-dependent kinase inhibitor 1	P38936	4/13	7.24	31119	38.3	Cell cycle regulatory
6	Rho-GTPase activating protein 4	P98171	9/22	3.73	27055	55.5	Signal transduction
7	S-phase kinase-associated protein 2	Q13309	7/11	3.97	77439	32.5	Cell cycle regulatory
8	Platelet membrane glycoprotein	P08514	5/12	3.62	38107	47.1	Signal transduction
9	Fibronectin	P02751	8/15	9.61	25933	52.6	Signal transduction
10	Cks1 protein	P61024	4/11	5.13	26214	61.9	Cell cycle regulatory

Differentially labelled proteins form 2D analysis were identified by MALDI-TOF peptide mass fingerprinting. The Swiss-Prot accession number, peptides matching, pI, molecular weight and % coverage of analysed peptides are shown for each protein; Proteins displaying an average fold-difference of ≥ 5 fold up (+) or down (−) regulation between pairs of conditions were considered as significant difference.

annotation of all the identified proteins is summarized in Table 1. Based on protein functions using information from the database of Swiss-Prot websites, 10 identified proteins associated with stable overexpression of let-7a were categorized into 3 protein groups. Most of the differentially expressed proteins were cell cycle regulators and proteins related to signal transduction or metabolism.

3.4. Identification of let-7a related proteins by Western blot analysis

To determine whether overexpressing let-7a in SGC-7901 has an effect on Cyclin-dependent kinase inhibitor 1, S-phase kinase-associated protein 2 and Fibronectin protein. Western blot analysis of the expression levels of these proteins was performed. The
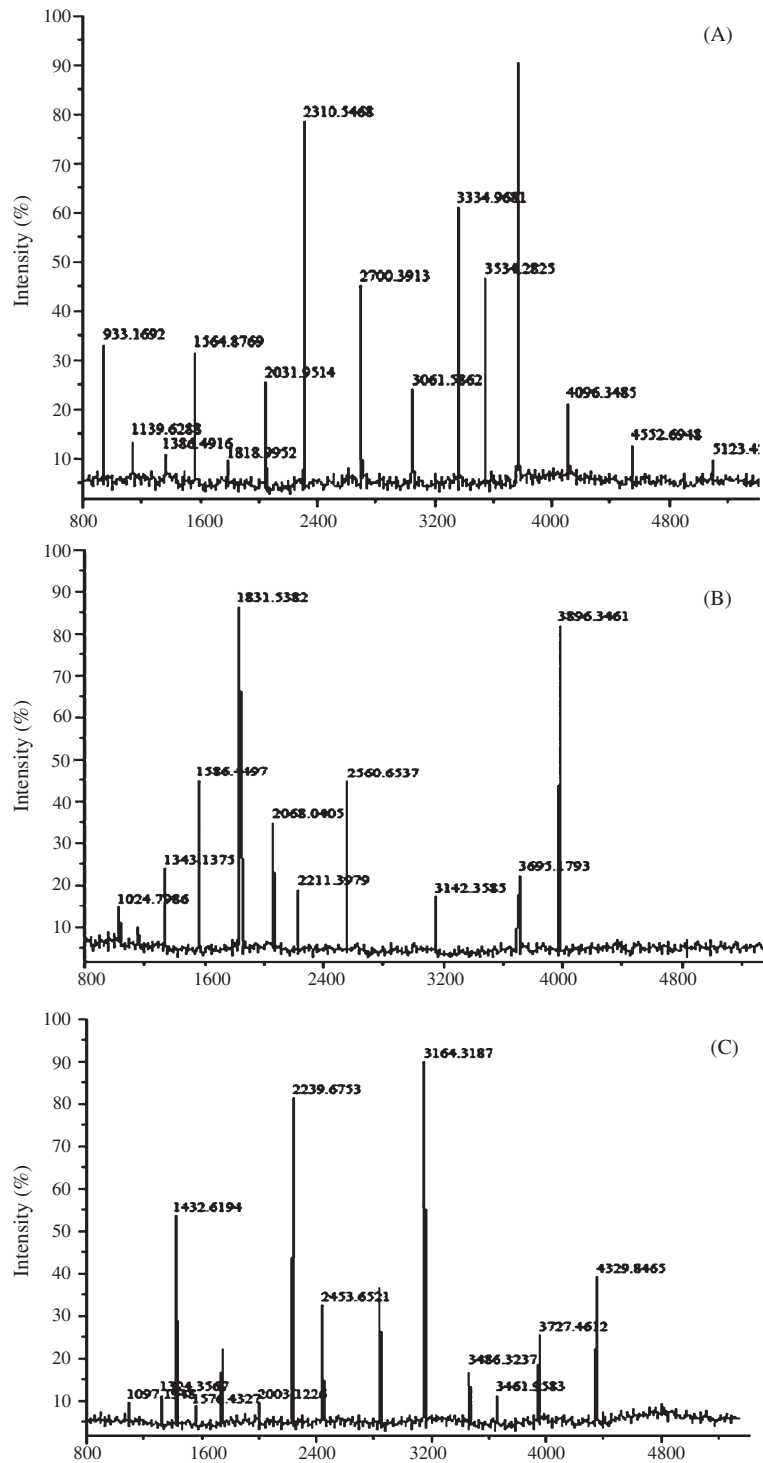
Fig. 5. MALDI-TOF-MS analysis of differential proteins. (A) MALDI-TOF-MS mass spectrum of spot 5 identified as CDKN1 according to the marched peaks was shown. (B) MALDI-TOF-MS mass spectrum of spot 7 identified as Skp2 according to the marched peaks was shown. (C) MALDI-TOF-MS mass spectrum of spot 9 identified as fibronectin according to the marched peaks was shown.
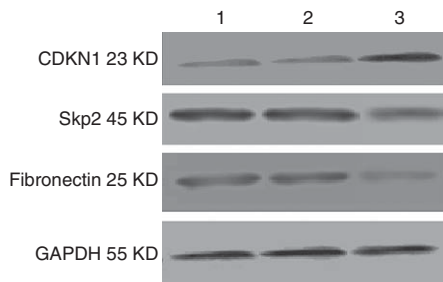
Fig. 6. Representative Western blot analysis of CDKN1, Skp2 and Fibronectin using GAPDH as internal control among SGC-7901, SGC-7901/EV and SGC-7901/let-7a cell lines. Compared with SGC-7901/EV and SGC-7901, SGC-7901/let-7a had obvious up-regulation of CDKN1, and a marked down-regulations of Skp2 and Fibronectin 1: SGC-7901; 2: SGC-7901/EV; 3: SGC-7901/let-7a.

results showed that in SGC-7901/let-7a cells, Cyclin-dependent kinase inhibitor 1 protein level significantly increased, while S-phase kinase-associated protein 2 and Fibronectin were reduced, compared to SGC-7901/EV and SGC-7901 cells ($P < 0.05$), as can be seen from the immunoblots shown in Fig. 6. The result verified that these differentially expressed proteins were related to let-7a in gastric carcinoma cells.

4. Discussion

This study combined a proteomic approach with gene therapy techniques to identify proteins associated with the function of let-7a in gastric carcinoma. We successfully used gene clone technology constructing the let-7a lentivirus and stably up-regulating let-7a gene expression in SGC-7901 cell line. As a reliable cell model, the well-resolved, reproducible 2-DE patterns of SGC-7901/let-7a, SGC-7901/EV, and SGC-7901 were established. Ten differentially expressed proteins spots among the three cell lines were identified by MALDI-TOF-MS. Antioxidant protein 2, Insulin-like growth factor binding protein 2, Protein disulfide isomerase A2, C-1-tetrahydrofolate synthase, Cyclin-dependent kinase inhibitor1, Rho-GTPase activating protein 4 were upregulated in SGC-7901/let-7a cells, while S-phase kinase-associated protein 2, Platelet membrane glycoprotein, Fibronectin, Cks1 protein were downregulated. Some of the differential expression proteins are known to be associated with the let-7a

function, and others may be novel proteins associated with let-7a function. These differential proteins could provide new clues to elucidate the mechanisms of let-7a in gastric carcinoma.

CDKN1, a protein that regulates cell cycle progression, terminal differentiation and apoptosis, mediates p53-dependent G1 growth arrest. Earlier studies supported the view that CDKN1 suppresses tumors by promoting cell cycle arrest in response to various stimuli. Additionally, substantial evidence from biochemical and genetic studies indicates that CDKN1 acts as a master effector of multiple tumour suppressor pathways for promoting anti-proliferative activities that are independent of the classical p53 tumor suppressor pathway [16, 17]. Skp2 is an F-box protein that plays a critical role in coordinating the G1/S transition and progression through the S phase of the mammalian cell cycle [18, 19]. It is mainly responsible for ubiquitylation and subsequent degradation of cell cycle regulators, and in particular the cell cycle inhibitor p27^{Kip1}. Fibronectin was discovered over thirty years ago as a protein abundantly secreted by tumor cells. Intense investigation of the function of fibronectin *in vitro* led to the discovery of integrins and other proteins involved cell motility and in the bi-directional communication between cells and their environment. Fibronectin is highly up-regulated around newly developing vasculature during embryogenesis and in pathological conditions including atherosclerosis, cardiac hypertrophy, and tumorigenesis. Recent genetic studies in fish, frogs and mice have suggested that fibronectin functions in maintaining or establishing cell polarity and its splice variants in development of vascular smooth muscle cells [20]. Cks1, a member of the highly conserved Suc1/Cks family of cell cycle regulatory proteins binds to Skp2 and promotes the association of Skp2 with p27 phosphorylated on Thr-187 [21]. The general notion that functional platelets are important for successful hematogenous tumor metastasis had been inaugurated more than 4 decades ago and has since been corroborated in numerous experimental settings. Pivotal preclinical experiments have demonstrated that hematogenous tumor spread was dramatically diminished when platelets were depleted from the circulation [22]. Cell migration affects all morphogenetic processes and contributes to numerous diseases, including cancer. The Rho GTPases regulate adhesion by directly controlling the balance between actin-mediated protrusion and myosin II-mediated contraction [23, 24].

Adhesion formation and disassembly drive the migration cycle by activating Rho GTPases, which in turn regulate actin polymerization and myosin II activity, and therefore adhesion dynamics. Insulin-like growth factor binding protein 2 (IGFBP-2) mRNA is already expressed in preimplantation embryos, and expression continues at high levels in many tissues during embryonic and fetal development. In the postnatal period, IGFBP-2 is the second most abundant IGFBP in the circulation and is present in various other biological fluids and tissues of many vertebrate species [25]. IGFBP-2 is overexpressed in many malignancies and is often correlated with an increasingly malignant status of the tumor, pointing to a potential involvement of IGFBP-2 in tumorigenesis. Antioxidant protein 2 (AOP2) is a novel thiol-dependent antioxidant that functions to scavenge particular hydroperoxides in the cell and mediate specific signals. There is also evidence supporting a role for AOP2 in certain disease processes including atherosclerosis. Further evaluation of this protein and its substrate specificity will likely shed light on its precise role in cellular oxidant defense, signal transduction and pathogenesis [26]. Protein disulfide isomerase (PDI) catalyzes protein folding and thiol-disulfide interchange reactions. The enzyme is localized in the lumen of endoplasmic reticulum (ER) and is abundant in secretory cells of various tissues [27]. C-1-tetrahydrofolate synthase was also differentially expressed in different human leukemia and lymphoma cell lines. This provided insights into the molecular basis of these malignancies and its role in cellular properties [28].

Considering the functions of the identified differential proteins, it is reasonable to predict that the proteins such as Cyclin-dependent kinase inhibitor 1, S-phase kinase-associated protein 2 and fibronectin are associated with the function of let-7a in SGC-7901. Introducing gene augmentation into proteomics revealed a novel let-7a signal pathway. These findings provide the basis to comprehensively investigate the functional mechanisms of let-7a in gastric carcinoma.

Acknowledgments

References

[1] R.S. Pillai, MicroRNA function: Multiple mechanisms for a tiny RNA? *RNA* **12** (2005), 1753–1761.

[2] P.D. Zamore and B. Haley, Ribo-gnome: The big word of small RNAs, *Science* **309** (2005), 1519–1524.

[3] B.P. Lewis, C.B. Burge and D.P. Bartel, Conserved seed pairing, often flanked by adenosines, indicates that thousands of human genes are microRNA targets, *Cell* **120** (2005), 15–20.

[4] C.M. Croce and G.A. Calin, microRNA, cancer, stem cell division, *Cell* **122** (2005), 6–7.

[5] C.Z. Chen, L. Li, H.F. Lodish and D.P. Bartel, MicroRNA modulate hematopoietic lineage differentiation, *Science* **303** (2004), 83–86.

[6] D. Didiano and O. Hobert, Perfect seed pairing is not a generally reliable predictor for microRNA–target interactions, *Nat Struct Mol Biol* **13** (2006), 849–851.

[7] N.R. Smalheiser and V.I. Torvik, Complications in mammalian microRNA target prediction, *Methods Mol Biol* **342** (2006), 115–127.

[8] Y.M. Zhu, Z.X. Zhong and Z.M. Liu, Significance and relationship between let-7a and gastric mucosa cancerization, *World J Gastroenterology* **16** (2010), 3325–3329.

[9] Y.M. Zhu, Z.X. Zhong and Z.M. Liu, Lentiviral vector-mediated upregulation of let-7a inhibits gastriccarcinoma cell growth *in vitro* and *in vivo*, *Scandinavian Journal of Gastroenterology* **46** (2011), 53–59.

[10] Y.M. Zhu, Z.M. Liu and W.B. Bai, Experimental study on the effect of let-7a in Cell cycle of human gastric carcinoma cell line, *Chinese Journal of Experimental Surgery* **16** (2010), 424.

[11] M.R. Wilkins, J.C. Sanchez and A.A. Gooley, Progress with proteome projects: Why all proteins expressed by a genome should be identified and how to do it, *Biotechnol Genet Eng Rev* **13** (1996), 19–50.

[12] Y. Sun, H. Yi and P.F. Zhang, Identification of differential proteins in nasopharyngeal carcinoma cells with p53 silence by proteome analysis, *FEBS Letters* **581** (2007), 131–139.

[13] B. Zhang, P. Metharom and H. Jullie, The significance of controlled conditions in lentiviral vector titration and in the use of multiplicity of infection (MOI) for prediction gene transfer events, *Genet Vaccines Ther* **2** (2004), 6.

[14] P.S. Bernard and C.T. Wittwer, Real-Time PCR technology for cancer diagnostics, *Clin Chem* **48** (2002), 1178–1185.

[15] G. Candiano, M. Bruschi and L. Musante, Blue silver: A very sensitive colloidal Coomassie G-250 staining for proteome analysis, *Electrophoresis* **25** (2004), 1327–1333.

[16] C. Deng, P. Zhang, J.W. Harper, S.J. Elledge and P. Leder, Mice lacking p21CIP1/WAF1 undergo normal development, but are defective in G1 checkpoint control, *Cell* **82** (1995), 675–684.

[17] I.B. Roninson, Oncogenic functions of tumour suppressor p21Waf1/Cip1/Sdi1: Association with cell senescence and tumour-promoting activities of stromal fibroblasts, *Cancer Lett* **179** (2002), 1–14.

[18] C. Catzavelos, N. Bhattacharya and Y.C. Ung, Decreased levels of the cell-cycle inhibitor p27Kip1 inhibitor protein: Prognostic implications in primary breast cancer, *Nat Med* **3** (1997), 227–230.

[19] V. Esposito, A. Baldi and A. De Luca, Prognostic role of the cyclin dependent kinase inhibitor p27 in non-small lung cancer, *Cancer Res* **57** (1997), 3382–3385.

[20] S. Astrof and R.O. Hynes, Fibronectins in vascular morphogenesis, *Angiogenesis* **12** (2009), 165–175.

[21] D. Sitry, M.A. Seeliger and T.K. Ko, Three different binding sites of Cks1 are required for p27-ubiquitin ligation, *J Biol Chem* **44** (2002), 42233–42240.

[22] L. Erpenbeck and M.P. Schon, Deadly allies: The fatal interplay between platelets and metastasizing cancer cells, *Blood* **115** (2010), 3427–3436.

[23] A.B. Jaffe and A. Hall, Rho GTPases: Biochemistry and biology, *Annu Rev Cell Dev Biol* **21** (2005), 247–269.

[24] J.T. Parsons, A.R. Horwitz, M. and A. Schwartz, Cell adhesion: Integrating cytoskeletal dynamics and cellular tension, *Nat Rev Mol Cell Biol* **11** (2010), 633–643.

[25] A. Hoeflich, R. Reisinger and H. Lahm, Insulin-like growth factor-binding protein 2 in tumorigenesis: Protector or promoter? *Cancer Res* **61** (2001), 8601–8610.

[26] S.A. Phelan, AOP2 (antioxidant protein 2): Structure and function of a unique thiol-specific antioxidant, *Antioxid Redox Signal* **1** (1999), 571–584.

[27] M.G. Desilva, J. Lu and G. Donadel, Characterization and chromosomal localization of a new protein disulfide isomerase, PDIp, highly expressed in human pancreas, *DNA Cell Biol* **15** (1996), 9–16.

[28] S. Gez, B. Crossett and R.I. Christopherson, Differentially expressed cytosolic proteins in human leukemia and lymphoma cell lines correlate with lineages and functions, *Biochim Biophys Acta* **1774** (2007), 1173–1183.